

Flow Modelling in Long Surface Patterned Micromixers Using Division in Multiple Geometrical Subunits

Joshua Clark¹, Tahir A. Butt¹, Gautam Mahajan², Chandrasekhar R. Kothapalli², ¹Miron Kaufman and Petru S. Fodor^{*1}

¹Physics Department, Cleveland State University

²Chemical and Biomedical Engineering Department, Cleveland State University

*Corresponding author: Department of Physics, Cleveland State University, 2121 Euclid Avenue, Cleveland, OH 44236, p.fodor@csuohio.edu

Abstract: Optimization of mixing in microfluidic devices is a popular application of computational fluid dynamics software packages, such as COMSOL Multiphysics, with an increasing number of studies being published on the topic. However, it has to be noted that even very performant mixing topologies, such as the use of ridge-groove surface features, require multiple mixing units. This in turn requires very high resolution meshing, in particular when looking for solutions for the convection-diffusion equation governing the reactant or chemical species distribution. For the typical length of microfluidic mixing channels, analyzed using finite element analysis, this becomes computationally challenging due to the large number of elements that need to be handled. In this work we describe a methodology using the COMSOL 5.3a Computational Fluid Dynamics and Chemical Reaction Engineering modules, in which large geometries are split into subunits, allowing the governing equations to be evaluated on much higher resolution meshing. A comparison between the solutions obtained on global models and models split into subunits illustrates that much finer details can be observed in the later.

Keywords: micromixing, CFD, surface patterned micromixers, staggered herringbone mixers (SHB)

1. Background

In recent decades microfluidic devices have garnered attention as transforming technologies for chemical and biological synthesis and assays, due to their portability, minimal use of reagents, increased control over reaction conditions, and the possibility for easier scalability from prototypes to large scale applications [1]. One of the basic operations that almost every microfluidic device has to achieve is mixing, as essentially any of their applications in reaction engineering or analysis relies on two reagents being brought in close proximity [2]. In order to control and enhance mixing, many micro-scale mixing configurations rely on the pressure differential between the inlet and outlet of the device and strategically placed geometrical structures to

either laminate/segment the fluid flow or induce cross-sectional transport. This in turn reduces the average distance over which the diffusion has to act in order to homogenize the system.

In the context of micro-scale mixing studies, numerical modeling of the fluid flow, concentration distribution and reaction kinetics, has proved a very effective tool for guiding the design of effective mixing strategies. On these scales the fluid flow is laminar and microfluidic simulations have allowed for accurate numerical modeling of fluid motion and particle distributions in a wide range of geometrical configurations of varying complexity. However, the same laminar nature of these flows presents problems in applications involving mixing. Thus, the designers of microfluidic systems are forced to develop strategies focused on inducing mixing at the microscale by altering various geometrical parameters and flow rates and identifying optimal designs. Since complete mixing typically requires the use of multiple mixing units, the quality of the numerical solutions is heavily dependent on the mesh resolution used in the simulation. In this study, we show how one can partition a full microchannel geometry into distinct subunits and solve the global problem sequentially, in an effort to increase the overall resolution of the numerical solution. We will describe in full detail how to accomplish this using the Chemical Engineering module in COMSOL Multiphysics 5.3a, and we will compare the numerical findings to some experimental results with the purpose of highlighting the quality of numerical solutions acquired through iterative solving methods.

2. Microchannel Geometry

The micromixer geometry studied in this work is based on the strategy of patterning the surface of straight channels with an array of slanted ridges and grooves. Systems of ridge-grooves (Figure 1) following either a periodic pattern, also known as staggered herring bone (SHB) pattern [3,4], or a pattern generated based on a fractal algorithm [5, 6] are used as control features for the fluid flow.

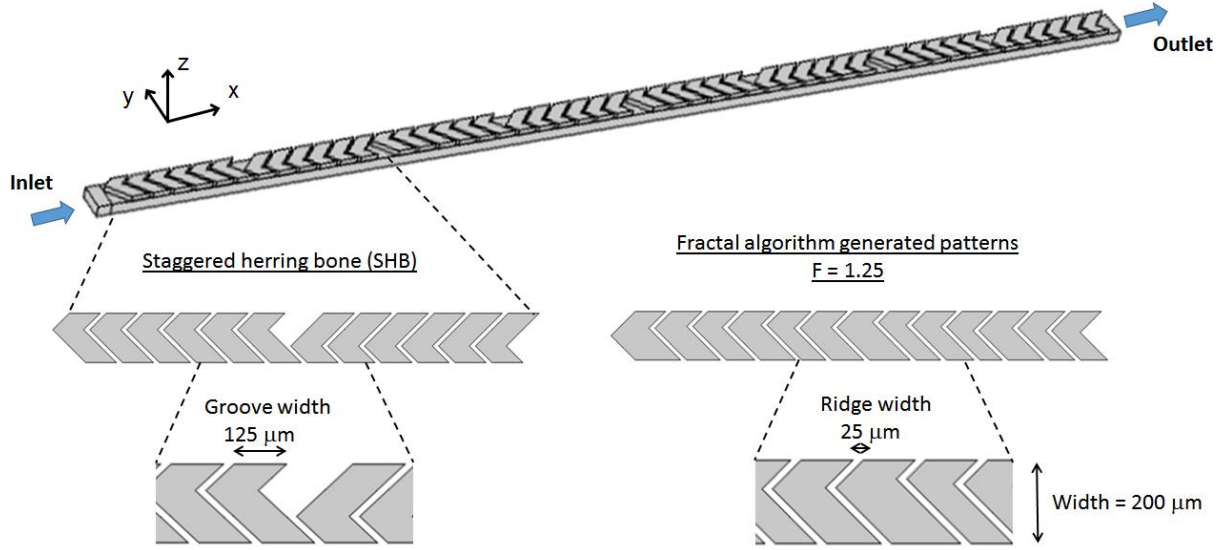


Figure 1. General topology of the micromixers investigated; (left) Snapshot of the ridge/groove profile of a full mixing unit for an SHB design; (right) Snapshot of the ridge/groove profile for a mixing section generated based on the Weierstrass function.

Channels such as these are particularly popular due to their solid performance and their relatively simple manufacturability using soft-lithography and replica molding. The design uses shallow angled ridges-grooves to generate traversal flows capable of inducing mixing. For the SHB design (Figure 1a), the apex of these angled grooves alternates between the inner and outermost thirds of the width of the channel, with every set consisting of six grooves. For the non-periodic design (Figure 1b), the apex locations are defined using a Weierstrass function:

$$W(x) = \sum_{n=0}^{\infty} \frac{\sin(2^n x)}{2^{n(2-F)}} \quad [1]$$

where F is the fractal dimension. By using the fractal Weierstrass algorithm one can reliably generate any number of identical copies of a chaotic/random looking mixer. In both designs, each groove is $125 \mu\text{m}$ in width and $33 \mu\text{m}$ in depth, and is spaced $25 \mu\text{m}$ away from the next groove. The primary channel is $66 \mu\text{m}$ in height and has a width of $200 \mu\text{m}$.

3. Numerical Model

Numerical solutions are generated using the Computational Fluid Dynamics and Chemical Engineering modules in COMSOL Multiphysics 5.3a. The flow fields are found by solving the Navier-Stokes equations for an incompressible Newtonian fluid in a steady-state pressure-driven flow:

$$\rho \left[\frac{\partial \mathbf{u}}{\partial t} + (\mathbf{u} \cdot \nabla) \mathbf{u} \right] = -\nabla p + \eta \nabla^2 \mathbf{u} \quad [2]$$

$$\nabla \cdot \mathbf{u} = 0 \quad [3]$$

where ρ ($\text{kg}\cdot\text{m}^{-3}$) is the fluid's density, \mathbf{u} ($\text{m}\cdot\text{s}^{-1}$) is the velocity, P (Pa) is the pressure, η ($\text{kg}\cdot\text{m}^{-1}\cdot\text{s}^{-1}$) is the fluid's viscosity, and t (s) is time. No-slip boundary conditions are set for the walls of the channel's geometry. The pressure at the outlet is set to zero, while the average fluid velocities at the inlet are set in a range 0.085 m/s to 0.85 m/s corresponding to Reynolds numbers in the range $\text{Re} = 10 - 100$. The working fluid is chosen to be water.

Subsequently the flow field solutions are then used to calculate the species concentration throughout the channel by solving the convection-diffusion equation:

$$\frac{\partial c}{\partial t} = D \nabla^2 c - \mathbf{u} \cdot \nabla c \quad [4]$$

where c ($\text{mol}\cdot\text{m}^{-3}$) is the species concentration, and D ($\text{m}^2\cdot\text{s}^{-1}$) is the coefficient of diffusion. Equation (4) is derived for an incompressible fluid, using Equation (3). The two chemical components to be mixed are introduced on separate halves of the inlet using step-like concentration profiles aligned with the median of the inlet. The maximum concentration is set to 1 mol/m^3 and the diffusion constant is set to $1 \times 10^{-9} \text{ m}^2\cdot\text{s}^{-1}$, which is typical for the diffusion of ions in aqueous solutions.

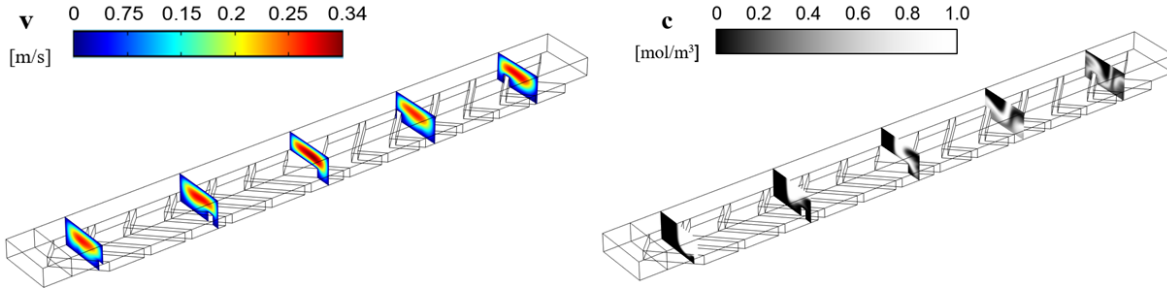


Figure 2. Velocity (left) and concentration (right) solutions in the SHB type micromixer ($Re=20$).

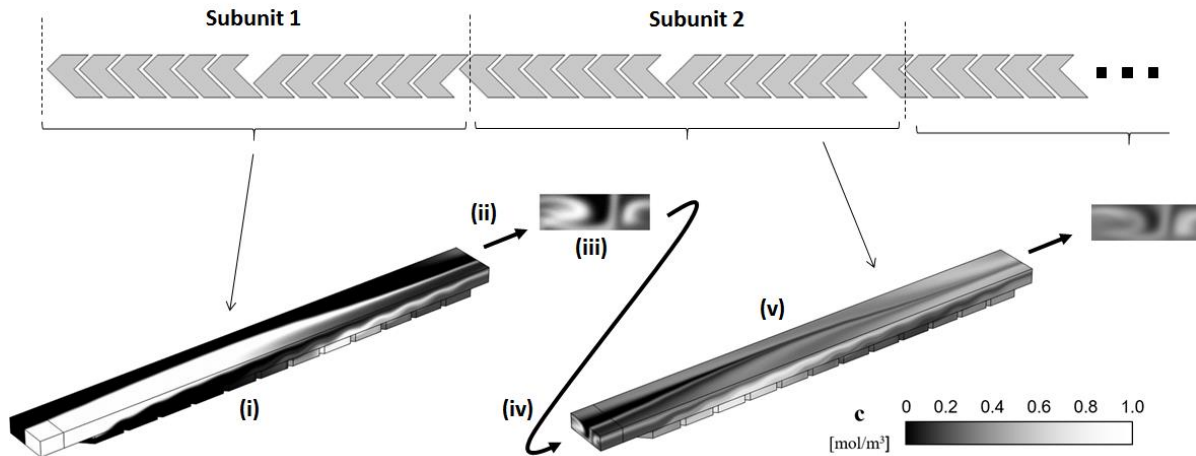


Figure 3. Process layout for solving large geometries by segmentation into subunits. Each step (i) to (v) is described in the text.

Both the flow fields and the concentration equations are solved using a geometrical multigrid GMRES iterative solver with a geometrical multigrid pre-conditioner and a Vanka algorithm for pre- and post-smoothing. For both numerical problems, a tetrahedral mesh is used, generated using the automatic meshing embedded in COMSOL.

4. Problem Segmentation

Typical evolutions of the flow field and concentration maps along one mixing unit of an SHB design, obtained using the above numerical models are shown in Figure 2. For all the modeling work presented, a workstation with a processor Intel Core i5 – 8400 with 32 Gb of RAM was used. It has to be noted though that even with a performant hardware platform, as more mixing units are added to the system, the quality of the numerical results progressively diminishes. This is due to the need to make the meshing rougher to accommodate the increase in the volume that has to be covered. In particular when solving the mass transport problem, if the number of elements used to discretize the geometry of interest is not large enough, large

numerical errors can accumulate and corrupt the results [7].

To address this issue, the geometry of interest, in this case the long channel micromixers, is partitioned into smaller geometrical units, each saved into a separate COMSOL model file. For example, for the SHB design, which is periodic, a natural choice for the subunit is a full mixing unit consisting of 6 grooves with the apex aligned at $y = -66 \mu\text{m}$ with respect to the median of the channel, followed by 6 grooves with the apex aligned at $y = 66 \mu\text{m}$. Subsequently the procedure illustrated in Figure 3 is followed:

- (i) The Navier-Stokes and concentration-diffusion equations are solved for the first geometrical unit of the channel, with the desired inlet boundary conditions, i.e. the chosen flow rates and step concentration profiles for the components to be mixed.
- (ii) Once the solution is obtained, a “Cut Plane” section is generated in the “Results” tab, near the outlet. While, the cut plane is parallel to the outlet, it is a few mesh elements away from it, to avoid the interpolation at the boundary to affect the data to be exported.

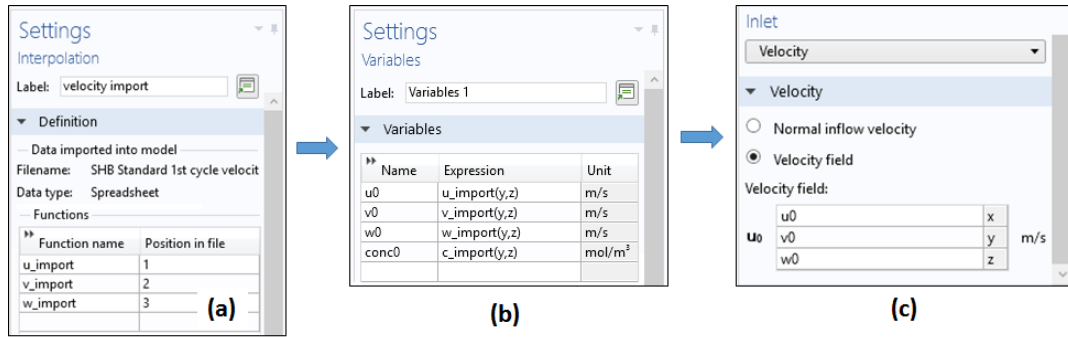


Figure 4. (a) Definitions of the interpolation functions in the model for subsequent cycles; (b) Definition of variables to define the boundary conditions for the inlet; (c) Mapping the outlet of one cycle on the inlet of the next cycle.

- (iii) Subsequently, the “Export” feature is used to save the data across the plane generated in step (ii), for the velocity components (u , v , w) and the concentration c , respectively. Each resulting exported text-based file contains aside from the variables of interest the two spatial coordinates across the cut-plane. The output for the export operation is set for an evaluation on a “rectangular grid” with a number of points exceeding the number of grid points in the mesh used for the mass transport equation solution.
- (iv) The data thus obtained at the outlet of one cycle is used as the inlet condition for the next cycle. To achieve this, in the model corresponding to the next cycle, under the “Definitions” tab two interpolation functions are generated that use the data generated in Step (iii) for the velocities and concentration (Figure 4a). These interpolation functions are then used to define a new set of variables ($u0$, $v0$, $w0$, $c0$) (Figure 4b) that allow the mapping of the velocities and concentration onto the inlet of the new cycle (Figure 4c).
- (v) The inlet conditions for the new cycle are thus set, and the model can be solved to obtain the flow field and concentration distribution. Subsequently, steps (ii) through (v) can be repeated to obtain the velocity and concentration along extensive mixing systems.

5. Results and Discussion

The above procedure was tested on a SHB micromixer with 4 mixing units. First, a geometric model was built for the entire system with all the mixing units present. The flow fields and concentration distributions were numerically determined for this unsegmented system, using the maximum possible meshing for our hardware combination, that resulted in $\sim 3 \times 10^6$ domain elements for the solution to the laminar flow physics

interface and $\sim 11 \times 10^6$ domain elements for the solution to the transport of diluted species physics interface.

Following this the same problem was solved in a segmented mode in which the geometry was split into 4 separate mixing units and the procedure described in Section 4 above was applied. Figure 5 shows representative snapshots of the cross-sectional concentration distributions obtained with the two methodologies. While qualitatively the two concentration distributions look similar, it is immediately apparent that the level of detail achievable in the segmented models is much higher. In particular, one can easily identify the filaments that are characteristic to the counter-rotating transversal flows that are induced in these structures by the ridge-groove system [3-6]. These are important in reducing the distance over which molecular diffusion has to act in order to mix the different components and are critical to the efficiency of these mixers.

While in the above example the procedure has been applied in the context of a periodic structure such as the SHB design, a similar procedure can be applied to non-periodic structures, such as the ridge-groove system generated using a fractal sequence, in which no two subunits of the channel are identical. In this case each model in the sequence, has a different geometry, but the same procedure is used to map the solutions from the outlet of a subunit to the inlet of the next one. To this end the grayscale image in Figure 6, shows computational modeling results for a ridge-groove mixer generated based on a fractal sequence using Equation 1 with a fractal dimension $F = 1.25$. The total length of the mixer modeled is ~ 8 mm, equivalent with four complete mixing units of the SHB type design. Based on the above method the geometry was split into four distinct sections for the numerical analysis.

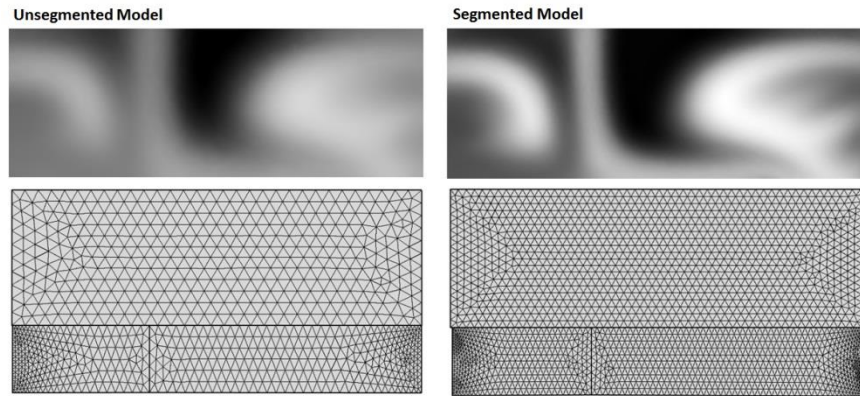


Figure 5. Concentration mapping results for a SHM mixers, numerically modeled using a global unsegmented geometry (left) and a segmented geometry (right) in which each mixing unit is modeled separately. Examples of the meshing achievable in each case are given. For the unsegmented geometry the average size of the mesh element is about $W/30$, while for the segmented geometry is about $W/60$, where W is the width of the channel.

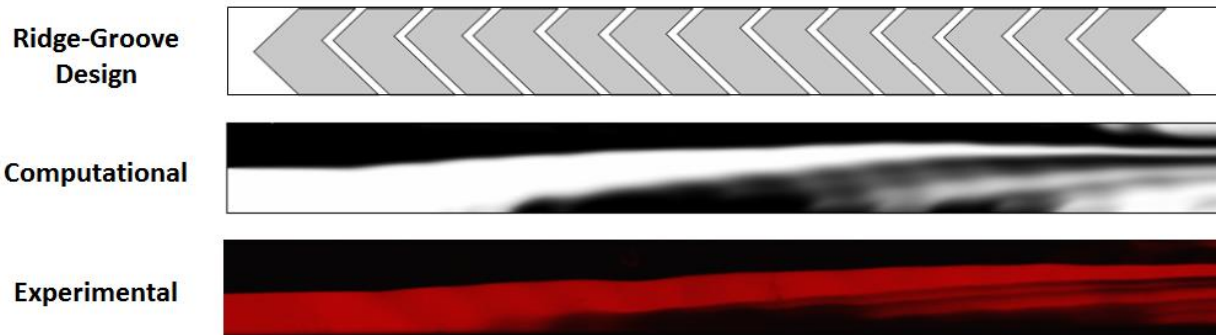


Figure 6. (Top) Ridge-groove design section for a micromixers generated using the fractal algorithm with $F = 1.25$; (middle) the corresponding concentration distribution along the micromixer obtained numerically ($Re = 20$, $z = 30 \mu\text{m}$ above the top of the ridges); (bottom) confocal image of dextran dye distribution in an experimental prototype with the same ridge-groove structure and same flow conditions.

These results are compared with experimental results obtained by doing confocal microscopy imaging on a prototype of the numerically modeled micromixer. The prototype was fabricated using standard soft-lithography methods [4, 8]. The imaging was performed using a Nikon A1 Rsi confocal microscopy system. For the above result, the distribution of a fluorescent dye solution $10 \mu\text{M}$ of 10 kDa rhodamine B-dextran introduced only on one side of the micromixer using a two-inlet system was monitored. As illustrated in the figure, good qualitative correlation between the numerical and experimental results is achieved.

6. Conclusions

In this work we have outlined a partitioning method that allows one to construct high-resolution numerical models for flow and mass transport

problems. The method relies on splitting large geometries into smaller subunits that are solved sequentially according to the direction of the flow. This allows one to circumvent hardware limitations for problems that are otherwise too large to solve with a large level of discretization. While the method was illustrated for a fluid dynamics case study, it has potential to be used in other transport problems, such as charge transport.

References

1. G.S. Geong, S. Chung, C.B. Kim, Applications of micromixing technology, *Analyst* 135, 460-473 (2010).
2. N.-T. Nguyen, *Micromixers: Fundamentals, Design and Fabrication*, 2nd edition; Elsevier: Oxford, UK, 2012.

3. A.D. Stroock, S.K.W. Dertinger, A. Ajdari, I. Mezic, H.A. Stone, G.M. Whitesides, Chaotic mixer for microchannels, *Science* 295, 647–651, (2002).
4. B. Hama, G. Mahajan, P.S. Fodor, M. Kaufman, R. Kothapalli, Evolution of mixing in a microfluidic reverse-staggered herringbone micromixer, *Microfluid. Nanofluid.* 22, 54 (2018).
5. M. Camesasca, M. Kaufman, I. Manas-Zloczower, Staggered passive micromixers with fractal surface patterning. *J. Micromech. Microeng.* 16, 2298-2311 (2006).
6. P.S. Fodor, M. Itomlenskis, M. Kaufman, Assessment of Mixing in Passive Microchannels with Fractal Surface Patterning, *European Physical Journal: Applied Physics* 47, 31301 (2009).
7. D. Kuzmin, A guide to numerical methods for transport equations, Friedrich-Alexander-Universität Erlangen-Nürnberg, Erlangen, Germany, 2010.
8. C.-W. Tsao, Polymer Microfluidics: Simple, Low-Cost Fabrication Process Bridging Academic Lab Research to Commercialized Production, *Micromachines* 7, 225 (2016)

Acknowledgements

This work has been partially supported by the National Science Foundation (NSF) under Grant No. 1659541 and by Cleveland State University (CSU) under the University Summer Undergraduate Research 2018 award. The confocal imaging of the microchannels has been done at the CSU fluorescence microscopy facility funded by the National Institute of Health (NIH) under Grant No. 1-S10-OD010381. Any opinions, findings, and conclusions or recommendations expressed in this material are those of the author(s) and do not necessarily reflect the views of the NSF, NIH, and CSU.